2016-01-11

A new method for the rapid analysis of 1H-Pyrrole-2,5-diones (maleimides) in environmental samples by two-dimensional gas chromatography time-of-flight mass spectrometry (GCGC-ToF-MS)

Naeher, S

http://hdl.handle.net/10026.1/4225

10.1016/j.chroma.2016.01.026
Journal of Chromatography A
Elsevier BV

Title: A new method for the rapid analysis of 1*H*-Pyrrole-2,5-diones (maleimides) in environmental samples by two-dimensional gas chromatography time-of-flight mass spectrometry

Author: Sebastian Naeher Sabine K. Lengger Kliti Gricea

PII: S0021-9673(16)00058-3
DOI: http://dx.doi.org/doi:10.1016/j.chroma.2016.01.026
Reference: CHROMA 357219

To appear in: *Journal of Chromatography A*

Received date: 4-11-2015
Revised date: 11-1-2016
Accepted date: 11-1-2016

A new method for the rapid analysis of 1*H*-Pyrrole-2,5-diones (maleimides) in environmental samples by two-dimensional gas chromatography time-of-flight mass spectrometry

Sebastian Naeher [a,*], Sabine K. Lengger [a,1], Kliti Grice [a,*]

[a] *Curtin University, Western Australia Organic and Isotope Geochemistry Centre (WA-OIGC), Department of Chemistry, The Institute for Geoscience Research, GPO Box U1987, Perth, WA 6845, Australia*

* Corresponding authors. Tel.: +61 8 9266 2474.

E-mail addresses: Sebastian.Naeher@curtin.edu.au (S. Naeher); K.Grice@curtin.edu.au (K. Grice)

[1] Present addresses: University of Bristol, Organic Geochemistry Unit, School of Chemistry, Cabot Institute, Cantock's Close, Bristol BS8 1TS, UK and University of Plymouth, Petroleum and Environmental Geochemistry Group, Biogeochemistry Research Centre, Drake Circus, Plymouth PL4 8AA, UK

Highlights:

- Improved simplicity and accuracy of analysis of maleimides by GC×GC-ToF-MS
- High sensitivity of the method enabled detection of new compounds
- Previous erroneous quantification due to coelution discovered
- Enable studies on environmental significance of chlorophyll degradation products

ABSTRACT

Maleimides (1*H*-Pyrrole-2,5-diones) are monopyrrolic pigment derivatives with specific alkyl side chains that can be directly linked to their tetrapyrrole precursors, most notably chlorophylls and bacteriochlorophylls. These compounds can be used as palaeoenvironmental indicators such as, for instance, algal productivity and redox conditions in ancient and modern aquatic systems. Here, we present a new method using two-dimensional gas chromatography time-of-flight mass spectrometry (GC×GC-ToF-MS), which enables the rapid analysis of maleimides in complex mixtures and different matrices (e.g. sediments and soils), therefore largely simplifying the previous intricate maleimide purification protocol. This method also reduces the potential for bias associated with partial losses due to low recovery and the high volatility of maleimides. The maleimide distributions and concentrations obtained by GC×GC-ToF-MS were reproducible and in agreement with the previously used purification procedure followed by analysis with traditional gas chromatography

- mass spectrometry (GC-MS). The new method also resolved previously unrecognised, partial coelution of some maleimides with unknown compounds by quantification with the *m/z* 75 fragment ion. Furthermore, the higher sensitivity enabled the detection of previously unrecognised and preliminarily identified maleimides based on their relative retention times. The new, easier, rapid and more sensitive GC×GC-ToF-MS method greatly facilitates the analysis of maleimides in environmental samples to study tetrapyrrole degradation processes and will further the development of maleimides as biomarkers for palaeoenvironmental reconstructions.

Keywords: maleimide; tetrapyrrole; chlorophyll; gas chromatography; GC-MS; GC×GC-ToF-MS

1. Introduction

Tetrapyrrole pigments comprise chlorophylls and bacteriochlorophylls, which are essential light absorbing and energy-transferring compounds for oxygenic and anoxygenic photosynthesis [e.g. 1,2]. Although these pigments have been intensely studied since the 1930s [3-7], improvements of analytical techniques during the last two decades have facilitated their characterisation in aquatic and terrestrial environments [e.g. 7]. Most notably, high performance liquid chromatography tandem mass spectrometry (HPLC-MS/MS) has enabled detailed investigations of pigments to reconstruct phototrophic communities in aquatic systems [e.g. 7,8,9-12].

Structural alteration and degradation processes of intact chlorophylls lead to a large variety of chlorin derivatives in the water column and sediments [e.g. 13,14-18]. The preservation of pigment derivatives during diagenesis and catagenesis allows reconstructions of ancient phototrophic community assemblages [e.g. 4,5,19-21].

Among degradation products of pigments are monopyrrolic derivatives (1*H*-Pyrrole-2,5-diones; maleimides; Fig. A1; [19]). These compounds have been used to study the structure and degradation processes of tetrapyrroles [e.g. 22,23-25]. Maleimides have also been detected in environmental samples, where they have been used as indicators of algal productivity, water column properties (i.e. redox conditions, stratification, chemocline depth) and depositional conditions [19,20,26-35]. However, the precursors of many maleimides have still not been fully identified, the processes leading to their formation are incompletely understood and their environmental significance needs further investigation [29].

Although maleimides can be analysed more easily than their precursor tetrapyrroles by gas chromatography due to their lower molecular weight, a relatively long, material and time consuming sample preparation and purification procedure comprising an array of silica gel column chromatography and thin layer chromatography is required to analyse maleimides in environmental samples [Section 2.2; 19,29]. Furthermore, this procedure might also introduce some bias such as losses of maleimides due to their high volatility and low recovery during separation and/or contributions from maleimides derived from the instability of tetrapyrroles during sample treatment.

In order to improve the current protocols and to facilitate the analysis of maleimides, we developed a rapid method to analyse maleimides based on two-dimensional gas chromatography (GC×GC) within lipid extracts and polar fractions from environmental samples.

GC×GC was first employed by Liu and Phillips [36] to increase chromatographic resolution of traditional one-dimensional gas chromatography, and has been extensively developed since then [e.g. 37,38], including coupling to mass spectrometers [39,40]. While GC×GC with flame ionisation detection (GC×GC-FID) has the advantage of improved peak shapes, a higher reproducibility and a more precise quantification, GC×GC coupled to time-of-flight mass spectrometry (GC×GC-ToF-MS) facilitates the determination of mass spectra and therefore the identification of biomarker compounds [37]. Major advantages of these instruments include direct analysis of organic compounds in complex mixtures and improved determination of labile and volatile molecules [41-44].

Here, we used recent sediment samples from a eutrophic lake in Switzerland and Devonian sedimentary rocks from a core section in the Canning Basin in Western Australia in order to compare ratios derived from conventional maleimide analysis (sample purification followed by GC-MS) and GC×GC-ToF-MS on clean fractions and total lipid extracts. Furthermore, we report the detection of novel maleimides based on relative retention times, distributions in the 2D chromatograms and mass spectra, measured by GC×GC-ToF-MS.

2. Material and methods

2.1. Study sites

Rock samples from the McWhae Ridge (Canning Basin, Western Australia; S 18°43.678 E 126°4.092, WGS84) were studied by [32,45,46]. The samples originate from a core section (MR-1 core; 27.2-42.1 m) which comprises the period between the Late Givetian (Middle Devonian) and the Middle to Late Frasnian (Late Devonian), and were investigated to reveal environmental changes before the Frasnian-Famennian boundary extinction event [32,45]. The geologic setting and information on the core section are summarised in [45]. In short, the lowest part of the section comprises the Gogo Formation (40.1-42.1 m), consisting of laminated argillaceous shales with thin limestone beds and irregular beds of wackestone and fine grained packstone. The following section (33.5-40.1 m) comprises calcareous siltstone with micrite nodules and argillaceous limestone. The uppermost part of the sampled section (27.2-33.5 m) consists of calcareous shale with narrow beds of micrite and packstone. Two samples from the core section were analysed, in depths of 27.88-28.25 m (MWR11) and 29.64-29.85 m (MWR13A).

The sediment sample from the Swiss Lake Rotsee (22-24 cm) originate from a 58 cm long core obtained with a gravity corer at the maximum depth of 16 m in August 2010 (N 47°4.251 E 8°18.955, WGS84). After recovery, the core was sliced into 2 cm intervals and frozen at -20 °C and freeze dried, ground and homogenised prior to analysis. The small (0.46 km^2) prealpine, monomictic and eutrophic Lake Rotsee is stratified most of the year with a chemocline between ca. 6 and 10 m and an anoxic hypolimnion [47]. Hydrographical and limnological parameters of this lake are summarised in [48]. The sedimentation rate is ca. 0.38 cm yr^{-1} [48], indicating that the core covers the last ca. 150 yr. The studied sample (22-24 cm) therefore corresponds to ca. 1947-1952. The biogeochemical history of the lake has been described previously [29,48-50].

2.2. Maleimide analysis

The rock samples from the McWhae Ridge (Canning Basin, Western Australia) were Soxhlet extracted as reported in [45]. In short, the rock samples were cut with a rocksaw and pre-extracted with methanol (MeOH) and dichloromethane (DCM) in an ultrasonic bath to remove potential surface contamination. After grinding the samples in a rock-mill, they were Soxhlet extracted with DCM/MeOH (9:1, v: v) for 48 h. Elemental sulfur was removed by activated copper. The total lipid extracts (TLEs) were separated by silica gel column chromatography into six fractions using *n*-hexane for saturated hydrocarbons, *n*-hexane/DCM (8:2, v: v) for aromatic hydrocarbons, *n*-hexane/DCM (1:1, v: v) for nickel porphyrins, DCM for vanadyl porphyrins, DCM/acetone (9.5:1, v: v) for maleimides (‘Si1 fraction’) and DCM/MeOH (1:1, v: v) to elute polar compounds. Half of the S1 fraction was used for direct analysis by GC×GC-ToF-MS, and the other half further purified as described below.

In contrast, the sediment sample from Lake Rotsee (Switzerland) was extracted by ultrasonication with DCM/acetone (1:1, v: v) and oxidised with 1.7% chromic acid (CrO_3) as described in [29]. The CrO_3 oxidised samples comprise naturally occurring maleimides as well as maleimides formed by oxidation of the tetrapyrroles within the extracts. An aliquot of the CrO_3-oxidised sample was separated by silica gel column chromatography into three fractions using DCM, 20% ethyl acetate (EtOAc) in DCM (i.e. ‘Si1 fraction‘, containing the maleimides; one aliquot was used for direct analysis by GC×GC-ToF-MS, another aliquot further purified as discussed below) and DCM/MeOH (1:1, v: v) [29].

In order to obtain maleimide fractions of sufficient purity for GC-MS analysis, aliquots of the Si1 fractions of the MWR and Lake Rotsee samples were subjected to preparative thin layer chromatography with 20% EtOAc in DCM as mobile phase [29]. H,H maleimide (Sigma Aldrich, 99%) was applied to each plate in parallel to the samples as retention standard. The band between ca. R_f 0.6 and 0.9 was recovered by elution with EtOAc on a short silica column. After derivatisation (overnight, room temperature) with 100 µL MTBSTFA [N-(*tert*-butyldimethylsilyl)-N-methyl trifluoroacetamide, Sigma Aldrich] in 150 µL pyridine to obtain TBDMS (*tert*-butyldimethylsilyl) derivatives, the carefully dried samples (under reduced pressure) were eluted with DCM over a short silica column and redissolved in *n*-hexane prior to analysis (purified fractions).

The analytical reproducibility of the separation and purification procedure was within 10% and 25% for the concentrations of Me,Et maleimide in the free and oxidised fractions, respectively, based on duplicate sample preparation and measurement of Lake Rotsee sediment by GC-MS.

The Si1 fractions were also derivatised with 100 µL MTBSTFA in 150 µL pyridine (overnight, room temperature), carefully dried under reduced pressure and redissolved in *n*-hexane prior to analysis.

Maleimides were named and abbreviated according to the nomenclature in [19,29]. Identification was based on relative retention times and published mass spectra [19,29,51] as well as authentic standards for H,H, Me,H, Me,Me, Et,H, Me,Et, Me,*i*-Pr, Me,*n*-Pr, Me,*neo*-Pent, CycloH, β-benzo and α-benzo maleimides provided by Y. Chikaraishi (JAMSTEC, Japan).

2.3. Instrumentation

The Si1 and purified fractions were analysed using two-dimensional gas chromatography-time-of-flight-mass spectrometry (GC×GC-ToF-MS). An Agilent 7890B GC system was used, fitted out for GC×GC with a LECO linear modulator, and coupled to a LECO Pegasus 4D time-of-flight mass spectrometer. The first dimension column (1D) was a Restek Rtx-5MS column [29 m x 0.25 mm inner diameter (i.d.) x 0.25 μm film thickness (f.t.)], whereas a Restek Rxi-17SILMS column (1.5 m x 0.18 mm i.d. x 0.18 μm f.t.) was used as second dimension column (2D). Helium was used as carrier gas with a constant flow of 1.05 mL min^{-1}. Splitless injection of samples (1 μL) was performed at an inlet temperature of 310 °C. The oven was programmed as follows: 40 °C (1 min isothermal), heated to 190 °C at 3 °C min^{-1}, then to 300 °C at 20 °C min^{-1}, isothermal at 300 °C for 10 min. The modulation period was 3 s, with a secondary oven offset of 40°C and a modulator offset of 15°C. The temperature of the transfer line to the ToF-MS was held at 290 °C, whereas the ion source temperature was 230 °C. The MS was operated in positive ion electron ionisation mode at 70 eV. The scan speed was 100 Hz with a range of *m/z* 35-650 Da. ChromaTOF (LECO) was used for data processing, with automatic baseline correction and peak detection matching against a library produced from mass spectra obtained from maleimides (from samples and standards).

For comparison, the purified fractions were also analysed using traditional one-dimensional gas chromatography mass spectrometry (GC-MS) on an Agilent 7890A system equipped with an Agilent DB-5MS column [60 m x 0.25 mm inner diameter (i.d.) x 0.25 µm film thickness (f.t.)] and coupled to an Agilent 5975C inert XL EI/CI MSD mass spectrometer using electron impact ionisation at 70 eV. The temperature program of the oven was 40 °C (1 min isothermal), 40 °C to 100 °C at 10 °C min^{-1}, 100 °C to 320 °C at 4 °C min^{-1}, isothermal at 320 °C for 30 min. The temperature of the transfer line to the MS was 280 °C and the ion source temperature was 230 °C. The inlet temperature was 250 °C. Helium was used as carrier gas with a constant flow of 1.2 mL min^{-1}. The scan range was *m/z* 50-650 Da. The software ChemStation was used for data processing. Samples (1 µL) were injected splitless.

Maleimides were quantified by coinjection with the TBDMS derivative of phthalimide (ca. 4 ng/injection) on both instruments, using the total ion current (TIC), *m/z* 75 and the base peaks of the respective maleimides as TBDMS derivatives ($[M - C_4H_9]^{+\cdot}$; *m/z* 154 for H,H; *m/z* 168 for Me,H; *m/z* 182 for Me,Me and Et,H; *m/z* 196 for Me,Et; *m/z* 194 for Me,vinyl; *m/z* 210 for Me,*i*-Pr, Et,Et, Me,*n*-Pr and H,*n*-Bu (suggested structure); *m/z* 224 for Et,*i*-Pr (suggested structure), Et,*n*-Pr (suggested structure), Me,*i*-Bu, Me,*sec*-Bu, Me,*n*-Bu and H,*n*-Pent (suggested structure); *m/z* 238 for Me,*neo*-Pent, Me,*i*-Pent (isomers 1-3, suggested structure) and Me,*n*-Pent; *m/z* 204 for the phthalimide standard; *m/z* 208 for CycloH; *m/z* 218 for β-benzo and α-benzo; Table 1, Fig. A1). However, we only report relative concentrations in this study as no response factors were determined for the different maleimides and the phthalimide standard.

3. Results and discussion

3.1. Maleimide detection based on one- and two-dimensional chromatography

Maleimides were detected in the purified fractions of McWhae Ridge and Lake Rotsee samples by GC-MS analysis (Fig. 1). The compound with the most intense base peak in the studied samples was 2-methyl-3-ethyl-maleimide (Me,Et maleimide) (Fig. 1), in agreement with [29,32]. Furthermore, based on GC-MS analysis, other less abundant maleimides could be detected, which showed various alkyl side chain patterns as reported in [19,29,51] based on authentic standard compounds, relative retention times and/or mass spectra (Fig. 1). These maleimides were maleimide (H,H maleimide) 2-methyl-maleimide (Me,H maleimide), 2,3-dimethyl-maleimide (Me,Me maleimide), 2-ethyl-maleimide (Et,H maleimide), 2-methyl-3-vinyl-maleimide (Me,vinyl maleimide), 2-methyl-3-*iso*-propyl-maleimide (Me,*i*-Pr maleimide), 2-methyl-3-*n*-propyl-maleimide (Me,*n*-Pr maleimide), 2-methyl-3-*iso*-butyl-maleimide (Me,*i*-Bu maleimide), 2-methyl-3-*n*-butyl-maleimide (Me,*n*-Bu maleimide), 2-methyl-3-*iso*-pentyl-maleimide (Me,*i*-Pent maleimide), 2-methyl-3-*n*-pentyl-maleimide (Me,*n*-Pent maleimide), 2,3-diethyl-maleimide (Et,Et maleimide) and 2-ethyl-3-*n*-propyl-maleimide (Et,*n*-Pr maleimide).

2-methyl-3-*sec*-butyl-maleimide (Me,*sec*-Bu maleimide) could not be detected in the studied MWR and Lake Rotsee samples, despite a previous report of Me,*sec*-Bu maleimide in the sediment of this lake [29]. 2-methyl-3-*neo*-pentyl-maleimide (Me,*neo*-Pent maleimide) was only detected in the MWR samples.

α- and β-methylbenzomaleimide (α- and β-benzo) and tetrahydrobenzomaleimide (CycloH) were also detected in the MWR samples based on relative retention times and mass spectra of authentic standards, whereas CycloH was below the limit of detection and the other compounds were only present in traces in the Lake Rotsee samples.

The same maleimides could also be detected in the purified samples by GC×GC-ToF-MS (Figs. 2, 3). The 2D chromatograms showed very similar maleimide distributions and relative retention times in the first dimension compared to the GC-MS chromatograms (Figs. 1, 2, 3), as well as similar mass spectra (Figs. 4, S1, S2). As expected, the H,H, Me,H, Me,Me and Et,H maleimides eluted earlier than Me,Et maleimide in the first dimension, whereas Me,vinyl maleimide eluted after Me,Et maleimide (Figs. 2, 3). In the second dimension, the elution order was opposite, with H,H maleimide showing the highest retention time on the more polar, second column (2.45 s; Figs. 2,3). The differential retention of the maleimides on both columns resulted in specific peaks in the 2D chromatograms. The other maleimides grouped into three series with the base peaks *m/z* 210, 224 and 238 (Figs. 2,3).

Based on the elution order on a DB5-MS column as reported in [19,51] for GC-MS chromatograms, Me,*i*-Pr maleimide eluted prior to Et,Et and Me,*n*-Pr maleimides in the *m/z* 210 series, whereas in the *m/z* 224 series Et,*n*-Pr maleimide eluted prior to Me,*i*-Bu, Me,*sec*-Bu and Me,*n*-Bu maleimides (Fig. 1). Using a stationary phase of the same polarity, similar relative retention times in the first dimension and relative peak areas were achieved (Figs. 2, 3). Similarly, also Me,*n*-Pent maleimide eluted after Me,*neo*-Pent and Me,*i*-Pent maleimides in the *m/z* 238. Phthalimide eluted prior to CycloH, β-benzo and α- benzo in the first dimension of the GC×GC-ToF-MS and GC-MS analyses (Fig. 3).

3.2. Quantitative comparison of maleimide analysis using GC-MS and GC×GC-ToF-MS

Relative concentrations of maleimides in the studied samples were determined by coinjection with a phthalimide standard. Maleimides were quantified by gas chromatography using either flame ionisation detection or mass spectrometry, in the latter case using either the *m/z* 75 or base peak fragment due to the up to three orders of magnitude varying concentrations of maleimides in environmental samples [e.g. 19,29,32].

Here, we compared concentrations calculated relative to the phthalimide standard based on the total ion current (TIC), the *m/z* 75 or base peak fragment between the GC-MS and GC×GC-ToF-MS chromatograms (Fig. 5a, 5b, 5c). Despite differences in the fragmentation pattern and response of the studied compounds, quantification has previously been observed to be comparable between both instruments [41], and the concentrations were similar between the two instruments when base peak fragments for the maleimides ($[M - C_4H_9]^{+\cdot}$; Fig. 5c, 5d, 5e) were used. However, GC×GC-ToF-MS analysis revealed that other compounds showing an *m/z* 75 peak were coeluting with some of the maleimides, resulting in inaccurate quantification when TIC or *m/z* 75 was used. This was causing some large offsets between the determined concentrations comparing both instruments, using *m/z* 75 and TIC, but not when the base peak was used, especially in the *m/z* 224 and 238 series and partly also for Me,H and Me,Me maleimides (Fig. 6). Although the TIC and *m/z* 75 are considered more accurate for quantification of maleimides due to unknown response factors and differential mass discrimination of different fragments, both may result in an overestimation of concentrations by one-dimensional GC-MS analysis.

Due to the at least 10 times higher concentration of Me,Et maleimide (Figs. 1, 2) relative to other maleimides in the studied samples, the concentrations of less abundant maleimides under exclusion of Me,Et maleimide were used to compare both methods (Figs. 5a-5e). Maleimide concentrations in the purified MWR11 sample determined by GC×GC-ToF-MS *vs.* GC-MS showed slopes of 1.2, 0.6 and 1.0 and R^2 values of 0.69 (n=10; p<0.01), 0.92 (n=10; p<0.01) and 0.97 (n=10; p<0.01) on the basis of TIC, *m/z* 75 and base peaks, respectively (Fig. 5a, 5b, 5c), typically with a lower number of compounds detected by GC-MS relative to GC×GC-ToF-MS as discussed above.

The good agreement of the data determined by both instruments indicates a high comparability of the analysed maleimide concentrations. In contrast, in the purified MWR13A sample, no correlation was found for concentrations determined by both instruments using TIC and *m/z* 75 (data not shown), which was the result of significant coelution of unknown compounds with maleimides during GC-MS analysis (Fig. 6). However, using the base peaks of maleimides for quantification in this sample resulted in a slope of 1.1 and a R^2 value of 0.96 (n=10; p<0.01) when Me,Et maleimide was excluded (Fig. 5d), indicating a higher specificity of the base peaks of maleimides. For comparison, the purified Lake Rotsee sample (excluding Me,Et maleimide) was also characterised by a slope of 1.0 and a high R^2 value of 0.97 (n=12; p<0.01; Fig. 5e).

Maleimide concentrations of the purified MWR11 and MWR13A samples also followed a linear relationship if also Me,Et maleimide as determined by both instruments was included, however with a higher slope of 1.3 instead of 1.0 (Fig. 5f, 5g). While most maleimides were < 200 ng g^{-1} TOC (except Me,Et maleimide in both samples, Me,Me maleimide in the MWR11 sample), Me,Et maleimide reached a concentration of almost 8000 ng g^{-1} TOC in the purified MWR11 sample based on GC×GC-ToF-MS analysis. Although the R^2 value was similar in both cases (Fig. 5f, 5g), the higher slope indicates that such high concentrations represent limits in the linearity between both instruments and only more diluted samples should be analysed to obtain correct maleimide concentrations.

Despite the good agreement of both methods, a higher relative concentration of low molecular weight maleimides (especially H,H, Me,H and Me,Me maleimides) was observed based on their base peaks in the MWR and Lake Rotsee samples obtained by GC×GC-ToF-MS compared to GC-MS analysis, indicating a higher sensitivity than GC-MS analysis for these compounds. In contrast, the concentration of higher molecular weight maleimides in the purified MWR and Lake Rotsee samples (e.g. maleimides with base peaks *m/z* 224, 238) determined by GC-MS was slightly higher, indicating that GC-MS analysis is more sensitive for higher masses. These relations reflect differences in the mass spectrometers, resulting in different response and therefore slightly different relative concentrations.

3.3. Comparison of direct analysis of maleimides versus wet laboratory sample preparation and purification procedure

The direct analysis of Si1 fractions of the MWR samples by GC×GC-ToF-MS and comparison to the purified fractions allowed the re-assessment of the accuracy of the traditional laboratory procedure, which is a necessary pre-treatment prior to analysis with GC-MS. The comparison of maleimide distributions obtained in the Si1 and purified fractions of the MWR samples by GC×GC-ToF-MS reveals reproducible maleimide distributions similar to those of the purified fractions (Fig. 2). Correlations between maleimide concentrations between the Si1 and purified MWR11 fractions were conc(Si1) = 1.0 x conc(purified) + 4.0 (R^2=0.99, n=17; $p<0.01$; Fig. 5h), and between the Si1 and purified MWR13A fractions conc(Si1) = 1.3 x conc(purified) - 0.04 (R^2=0.98; n=12; $p<0.01$; Fig. 5i). This indicates significant losses in the absolute amounts of maleimides using the traditional procedure.

Despite a high correlation between concentrations in the Si1 and purified MWR11 fractions (Fig. 5h), the concentrations of most maleimides in the purified fraction of the MWR11 sample were up to 25% lower than the concentrations in the Si1 fraction, and the concentration of Me,H, Me,vinyl and Me,*n*-Pent maleimides was 60%, 54% and 47% lower, respectively, indicating significant losses of these compounds due to the laboratory procedure. In contrast, in the purified fraction of the MWR13A sample, Me,vinyl, Me,*i*-Pr and Et,Et concentrations were 84%, 35% and 34% lower than in the Si1 fraction.

The differences between these fractions may partly be explained by uncertainties in the analytical reproducibility of the extraction and separation procedure (within 10% for free fractions such as the studied MWR samples; Section 2.2). Also losses due to the high volatility of the low molecular weight maleimides (i.e. H,H and Me,H maleimides) and due to incomplete recovery can occur. In particular, the losses of Me,*n*-Pent maleimide may occur during column or thin layer chromatographic separation due to its larger size and lower polarity than other maleimides. Me,vinyl maleimide may easily be oxidised due to the presence of oxygen during sample preparation, resulting in its lower abundance in the purified samples.

3.4. Preliminary identification of new maleimides based on GC×GC-ToF-MS analysis

In addition to the previously reported maleimides, other peaks with almost identical mass spectra as these from known maleimides were detected by GC×GC-ToF-MS analysis (Fig. 3, Table 1). However, the mass spectra of TBDMS derivatives of maleimides (Figs. 4, S1, S2) only dominate by *m/z* 75 and a characteristic base peak [19,52]. This prevents further interpretations regarding the structure based on the mass spectra, and thus, structural assignments can only be assumed based on relative retention times.

The compound eluting prior to Et,*n*-Pr maleimide (Fig. 3, Table 1) was assigned as 2-ethyl-3-*iso*-propyl-maleimide (Et,*i*-Pr maleimide) based on its spectrum (*m/z* 75, 210) and retention times. In the *m/z* 238 series, four other peaks with similar mass spectra eluted prior to Me,*n*-Pent maleimides (Fig. 3, Table 1). One of these peaks was Me,*neo*-Pent maleimide, which was confirmed by an authentic standard (Section 2.2). The other peaks may be Me,*i*-Pent isomers and/or compounds such as 2-ethyl-3-*iso*-butyl-maleimide (Et,*i*-Bu maleimide) and 2-ethyl-3-*n*-butyl-maleimide (Et,*n*-Bu maleimide), but a structural identification of these compounds awaits further confirmation by co-injection with authentic standards which will be the focus of future studies. Therefore, we assigned these maleimides as Me,*i*-Pent(1) to Me,*i*-Pent(3), with the latter compound corresponding to the Me,*i*-Pent maleimide which could also be identified by GC-MS analysis.

Furthermore, peaks with higher retention times in the *m/z* 210, 224 and 238 series were present in GC-MS chromatograms, which were not identified previously (Fig. 3, Table 1). The compound dominated by a base peak at *m/z* 75 and the mass 210 eluting after Me,*n*-Pr maleimides was most likely 2-*n*-butyl-maleimide (H,*n*-Bu maleimide), and similarly, the compounds eluting after Me,*n*-Bu maleimide in the *m/z* 224 series and after Me,*n*-Pent maleimide in the *m/z* 238 series are most likely 2-*n*-pentyl-maleimide (H,*n*-Pent maleimide) and 2-*n*-hexyl-maleimide (H,*n*-Hex maleimide) based on their equal differences in retention times which is strong evidence for a homologous series of compounds (Fig. 3, Table 1).

These new compounds were partly present in low intensities in the SIM traces of *m/z* 210, 224 and 238 obtained by conventional GC-MS analysis (Fig. 1), but in very low abundance, which may explain why they have not yet been reported. The GC×GC-ToF-MS approach is more sensitive for the detection of less abundant maleimides. Moreover, tetrapyrrole precursors with the proposed structures are so far unknown, rendering interpretations regarding their sources, formation processes and environmental significance yet impossible.

Furthermore, in the MWR and Lake Rotsee samples, potential maleimides of higher molecular weights were detected: a series of *m/z* 252 and 266 with five and three peaks, respectively (Fig. 3, Table 1), which showed spectra similar to maleimides (Fig. S2). Relative intensities were lower than those of the peaks in the *m/z* 238 series. The most abundant compounds of these series were preliminarily identified as 2-methyl-3-*n*-hexyl-maleimide (Me,*n*-Hex) and 2-methyl-3-*n*-heptyl-maleimide (Me,*n*-Hep) based on their mass spectra and relative retention times, and could also be detected by GC-MS. The other, less abundant compounds of these series have so far not been interpreted.

The identification of maleimides discussed in this section remains preliminary as no reference compounds were available. Although the origin of such compounds is unknown based on structural reasons considering known chlorophylls, these maleimides may be derived from bacteriochlorophyll derivatives and porphyrins with extended alkyl chains [10,53,54]. In contrast, thermal cracking and alkylation processes as suggested for maleimides with alkyl side chains up to C_{11} in crude oils [52] are unlikely in the immature, recent lake samples [29] and the low maturity rock samples from the Canning Basin [45] analysed in this study. This first report of their occurrence and simplified detection method will enable further studies to determine their environmental significance.

4. Summary and conclusions

GC×GC-ToF-MS analysis allows determination of maleimides with improved simplicity and accuracy compared to the traditional method, as confirmed by the analysis of distributions and concentrations of maleimides in Devonian rock samples from the Canning Basin, Australia and recent sediments from the Swiss Lake Rotsee. Concentrations obtained using both instruments matched best using characteristic base peak fragments of the maleimides as using TIC or the more general mass *m/z* 75 resulted both in overestimation by GC-MS due to coelution. The improved, two-dimensional separation has enabled the analysis of maleimides in complex mixtures and matrices, which facilitated prior purification procedures and allowed the detection of previously unknown maleimides. More research is required to confirm maleimides with the proposed structural assignments. The simplified and rapid analysis of maleimides will allow to significantly increase the knowledge about maleimide formation, provenance and significance in the environment, facilitate the determination of the origin of maleimides and the assessment of transformation and degradation of chlorophylls and other pigment precursors in the environment. Furthermore, it will be possible to widely use maleimides as biomarkers to reconstruct past and present surface water environments, the composition of associated phototrophic communities and biogeochemical cycling in these environments.

Acknowledgements

This research project was funded by DFG Research Fellowship NA 1172/1-1 (Naeher), awarded by the German Research Council (Deutsche Forschungsgemeinschaft; DFG). Additional funding came from ARC Discovery Outstanding Research Award (Grice) and ARC LIEFP grant for GC×GC-ToF-MS (Grice). Svenja Tulipani (Curtin University) and Carsten J. Schubert (Eawag, Switzerland) are thanked for providing rock extracts and fractions, and sediment samples, respectively. Yoshito Chikaraishi (JAMSTEC, Japan) is thanked for providing authentic reference compounds (synthesised maleimides). We acknowledge Geoff Chidlow (Curtin University) for technical support with GC-MS analysis. Philippe Schaeffer and Pierre Adam (University of Strasbourg, France) and Martijn Woltering (CSIRO, Australia) are thanked for helpful discussions.

References

[1] H. Scheer, An overview of chlorophylls and bacteriochlorophylls, in: B. Grimm, R.J. Porra, W. Rüdiger, H. Scheer (Eds.), Chlorophylls and Bacteriochlorophylls - Biochemistry, Biophysics, Functions and Applications, Springer, The Netherlands, 2006, pp. 1-26.

[2] T.S. Bianchi, E.A. Canuel, Chemical Biomarkers in Aquatic Ecosystems, Princeton University Press, Princeton, USA, 2011.

[3] A. Treibs, Chlorophyll and heme derivatives in organic mineral materials, Angew. Chem. 49 (1936) 682-686.

[4] A.J.G. Barwise, I. Roberts, Diagenetic and catagenetic pathways for porphyrins in sediments, Org. Geochem. 6 (1984) 167-176.

[5] G.W. Hodgson, B. Hitchon, K. Taguchi, B.L. Baker, E. Peake, Geochemistry of porphyrins, chlorins and polycyclic aromatics in soils, sediments and sedimentary rocks, Geochim. Cosmochim. Acta 32 (1968) 737-772.

[6] N. Ohkouchi, Y. Nakajima, N.O. Ogawa, Y. Chikaraishi, H. Suga, S. Sakai, H. Kitazato, Carbon isotopic composition of the tetrapyrrole nucleus in chloropigments from a saline meromictic lake: A mechanistic view for interpreting the isotopic signature of alkyl porphyrins in geological samples, Org. Geochem. 39 (2008) 521-531.

[7] B.J. Keely, Geochemistry of chlorophylls, in: B. Grimm, R.J. Porra, W. Rüdiger, H. Scheer (Eds.), Chlorophylls and Bacteriochlorophylls - Biochemistry, Biophysics, Functions and Applications, Springer, Berlin, 2006, pp. 535-561.

[8] R.L. Airs, B.J. Keely, Atmospheric pressure chemical ionisation liquid chromatography/mass spectrometry of bacteriochlorophylls from Chlorobiaceae: characteristic fragmentations, Rapid Commun. Mass Spectrom. 16 (2002) 453-461.

[9] R.L. Airs, J.E. Atkinson, B.J. Keely, Development and application of a high resolution liquid chromatographic method for the analysis of complex pigment distributions, J. Chromatogr. 917 (2001) 167-177.

[10] M.A. Wilson, D.A. Hodgson, B.J. Keely, Atmospheric pressure chemical ionisation liquid chromatography/multistage mass spectrometry for assignment of sedimentary bacteriochlorophyll derivatives, Rapid Commun. Mass Spectrom. 19 (2005) 38-46.

[11] D.H. Mawson, J.S. Walker, B.J. Keely, Variations in the distributions of sedimentary alkyl porphyrins in the Mulhouse basin in response to changing environmental conditions, Org. Geochem. 35 (2004) 1229-1241.

[12] S.W. Wright, S.W. Jeffrey, R.F.C. Mantoura, C.A. Llewellyn, T. Bjornland, D. Repeta, N. Welschmeyer, Improved HPLC method for the analysis of chlorophylls and carotenoids from marine phytoplankton, Mar. Ecol. Prog. Ser. 77 (1991) 183-196.

[13] J.W. Louda, J. Li, L. Liu, M.N. Winfree, E.W. Baker, Chlorophyll-*a* degradation during cellular senescence and death, Org. Geochem. 29 (1998) 1233-1251.

[14] J.W. Louda, P. Mongkhonsri, E.W. Baker, Chlorophyll degradation during senescence and death-III: 3-10 yr experiments, implications for ETIO series generation, Org. Geochem. 42 (2011) 688-699.

[15] E.T. Furlong, R. Carpenter, Pigment preservation and remineralization in oxic coastal marine sediments, Geochim. Cosmochim. Acta 52 (1988) 87-99.

[16] H.J. Callot, Geochemistry of chlorophylls, in: H. Scheer (Editor), Chlorophylls, CRC Press, Boca Raton, 1991, pp. 339–364.

[17] T.S. Bianchi, J.E. Dibb, S. Findlay, Early diagenesis of plant pigments in Hudson River sediments, Estuar. Coast. Shelf Sci. 36 (1993) 517-527.

[18] P.J. Harradine, P.G. Harris, R.N. Head, R.P. Harris, J.R. Maxwell, Steryl chlorin esters are formed by zooplankton herbivory, Geochim. Cosmochim. Acta 60 (1996) 2265-2270.

[19] K. Grice, R. Gibbison, J.E. Atkinson, L. Schwark, C.B. Eckardt, J.R. Maxwell, Maleimides (1*H*-pyrrole-2,5-diones) as molecular indicators of anoxygenic photosynthesis in ancient water columns, Geochim. Cosmochim. Acta 60 (1996) 3913-3924.

[20] K. Grice, P. Schaeffer, L. Schwark, J.R. Maxwell, Changes in palaeoenvironmental conditions during deposition of the Permian Kupferschiefer (Lower Rhine Basin, northwest Germany) inferred from molecular and isotopic compositions of biomarker components, Org. Geochem. 26 (1997) 677-690.

[21] B.J. Keely, P.G. Harris, B.N. Popp, J.M. Hayes, D. Meischner, J.R. Maxwell, Porphyrin and chlorin distributions in a Late Pliocene lacustrine sediment, Geochim. Cosmochim. Acta 58 (1994) 3691-3701.

[22] A.J.G. Barwise, E.V. Whitehead, Separation and structure of petroporphyrins, Physics and Chemistry of the Earth 12 (1980) 181-192.

[23] R.K. Ellsworth, Gas chromatographic determination of some maleimides produced by the oxidation of heme and chlorophyll *a*, J. Chromatogr. 50 (1970) 131-134.

[24] W. Rüdiger, Recent chemistry and biochemistry of bile pigments, Angew. Chem. Int. Ed. 9 (1970) 473-480.

[25] J.J. Jen, G. MacKinney, On photodecomposition of chlorophyll in vitro-II. Intermediates and breakdown products, Photochem. Photobiol. 11 (1970) 303-308.

[26] M. Kozono, S. Nomoto, H. Mita, R. Ishiwatari, A. Shimoyama, 2-Ethyl-3-methylmaleimide in Tokyo Bay sediments providing the first evidence for its formation from chlorophylls in the present photic and oxygenic zone., Biosci., Biotechnol., Biochem. 66 (2002) 1844-1847.

[27] M. Kozono, S. Nomoto, H. Mita, A. Shimoyama, Detection of maleimides and their characteristics in Neogene sediments of the Shinjo basin, Japan., Geochem. J. 35 (2001) 225-236.

[28] A. Shimoyama, M. Kozono, H. Mita, S. Nomoto, Maleimides in the Cretaceous/Tertiary boundary sediments at Kawaruppu, Hokkaido, Japan., Geochem. J. 35 (2001) 365-375.

[29] S. Naeher, P. Schaeffer, P. Adam, C.J. Schubert, Maleimides in recent sediments – Using chlorophyll degradation products for palaeoenvironmental reconstructions, Geochim. Cosmochim. Acta 119 (2013) 248-263.

[30] R.D. Pancost, N. Crawford, S. Magness, A. Turner, H.C. Jenkyns, J.R. Maxwell, Further evidence for the development of photic-zone euxinic conditions during Mesozoic oceanic anoxic events, J Geol Soc London 161 (2004) 353-364.

[31] R.D. Pancost, N. Crawford, J.R. Maxwell, Molecular evidence for basin-scale photic zone euxinia in the Permian Zechstein Sea, Chem. Geol. 188 (2002) 217-227.

[32] S. Naeher, K. Grice, Novel 1*H*-Pyrrole-2,5-dione (maleimide) proxies for the assessment of photic zone euxinia, Chem. Geol. 404 (2015) 100-109.

[33] K. Grice, R.E. Summons, E. Grosjean, R.J. Twitchett, W.J. Dunning, S. Wang, M.E. Bottcher, Depositional conditions of the Northern onshore Perth basin (Basal Triassic), Austral. Petrol. Prod. Explor. Assoc. J. 1 (2005) 263-273.

[34] J.H. Whiteside, K. Grice, Biomarker Records Associated with Mass Extinction Events, Annual Review of Earth and Planetary Sciences 44 (in press).

[35] K. Grice, C. Cao, G.D. Love, M.E. Böttcher, R.J. Twitchett, E. Grosjean, R.E. Summons, S.C. Turgeon, W. Dunning, Y. Jin, Photic zone euxinia during the Permian-Triassic superanoxic event, Science 307 (2005) 706-709.

[36] Z. Liu, J.B. Phillips, Comprehensive two-dimensional gas chromatography using an on-column thermal modulator interface, J. Chromatogr. Sci. 29 (1991) 227-231.

[37] C. Eiserbeck, R.K. Nelson, C.M. Reddy, K. Grice, Advances in Comprehensive Two-Dimensional Gas Chromatography (GC×GC), in: K. Grice (Editor), Principles and Practice of Analytical Techniques in Geosciences, Chapter 12, The Royal Society of Chemistry, 2014, pp. 324-365.

[38] M. Adahchour, J. Beens, U.A.T. Brinkman, Recent developments in the application of comprehensive two-dimensional gas chromatography, J. Chromatogr. 1186 (2008) 67-108.

[39] G.S. Frysinger, R.B. Gaines, Comprehensive two-dimensional gas chromatography with mass spectrometric detection (GC × GC/MS) applied to the analysis of petroleum, J. High. Resolut. Chromatogr. 22 (1999) 251-255.

[40] M. van Deursen, J. Beens, J. Reijenga, P. Lipman, C. Cramers, J. Blomberg, Group-type identification of oil samples using comprehensive

two-dimensional gas chromatography coupled to a time-of-flight mass spectrometer (GC×GC-TOF), J. High. Resolut. Chromatogr. 23 (2000) 507-510.

[41] C. Eiserbeck, R.K. Nelson, K. Grice, J. Curiale, C.M. Reddy, Comparison of GC-MS, GC-MRM-MS, and GC×GC to characterise higher plant biomarkers in Tertiary oils and rock extracts, Geochim. Cosmochim. Acta 87 (2012) 299-322.

[42] C. Eiserbeck, R.K. Nelson, K. Grice, J. Curiale, C.M. Reddy, P. Raiteri, Separation of 18α(H)-, 18β(H)-oleanane and lupane by comprehensive two-dimensional gas chromatography, J. Chromatogr. 1218 (2011) 5549-5553.

[43] M. Adahchour, J. Beens, R.J.J. Vreuls, U.A.T. Brinkman, Recent developments in comprehensive two-dimensional gas chromatography (GC × GC): III. Applications for petrochemicals and organohalogens, TrAC, Trends Anal. Chem. 25 (2006) 726-741.

[44] P. Marriott, R. Shellie, J. Fergeus, R. Ong, P. Morrison, High resolution essential oil analysis by using comprehensive gas chromatographic methodology, Flavour Fragrance J. 15 (2000) 225-239.

[45] S. Tulipani, K. Grice, P.F. Greenwood, P. Haines, P. Sauer, A. Schimmelmann, R.E. Summons, A.E. Foster, M.E. Böttcher, T. Playton, L. Schwark, Changes in palaeoenvironmental conditions in Late Devonian Reef systems from the Canning Basin, WA: A biomarker and stable isotope approach, Gondwana Res. 28 (2015) 1500–1515.

[46] S. Tulipani, K. Grice, P.F. Greenwood, L. Schwark, M.E. Böttcher, R.E. Summons, C.B. Foster, Molecular proxies as indicators of freshwater incursion-driven salinity stratification, Chem. Geol. 409 (2015) 61-68.

[47] C.J. Schubert, F. Lucas, E. Durisch-Kaiser, R. Stierli, T. Diem, O. Scheidegger, F. Vazquez, B. Müller, Oxidation and emission of methane in a monomictic lake (Rotsee, Switzerland), Aquat. Sci. 72 (2010) 455-466.

[48] S. Naeher, R.H. Smittenberg, A. Gilli, E.P. Kirilova, A.F. Lotter, C.J. Schubert, Impact of recent lake eutrophication on microbial community changes as revealed by high resolution lipid biomarkers in Rotsee (Switzerland), Org. Geochem. 49 (2012) 86-95.

[49] S. Naeher, H. Niemann, F. Peterse, R.H. Smittenberg, P.K. Zigah, C.J. Schubert, Tracing the methane cycle with lipid biomarkers in Lake Rotsee (Switzerland), Org. Geochem. 66 (2014) 174-181.

[50] S. Naeher, F. Peterse, R.H. Smittenberg, H. Niemann, P.K. Zigah, C.J. Schubert, Sources of glycerol dialkyl glycerol tetraethers (GDGTs) in catchment soils, water column and sediments of Lake Rotsee (Switzerland) – Implications for the application of GDGT-based proxies for lakes, Org. Geochem. 66 (2014) 164-173.

[51] K. Grice, Distributions and stable carbon isotopic compositions of individual biological markers from the Permian Kupferschiefer (Lower Rhine Basin, N.W. Germany), PhD thesis, University of Bristol, UK, Bristol, 1995.

[52] J.M.E. Quirke, G.J. Shaw, P.D. Soper, J.R. Maxwell, Petroporphyrins-II. The presence of porphyrins with extended alkyl substituents, Tetrahedron 36 (1980) 3261-3267.

[53] R. Baltenweck-Guyot, R. Ocampo, Identification of a novel 7-desmethyl-7-acetonyl bacteriophaeophorbide *c* series in a recent sediment, Org. Geochem. 38 (2007) 1580-1584.

[54] A.H. Squier, D.A. Hodgson, B.J. Keely, Sedimentary pigments as markers for environmental change in an Antarctic lake, Org. Geochem. 33 (2002) 1655-1665.

Figure captions

Fig. 1. Selected ion chromatograms obtained by gas chromatography – mass spectrometry (GC-MS) with maleimides detected in a) extract of McWhae Ridge rock sample MWR11 (purified fraction) and b) CrO_3 oxidised extract of Lake Rotsee sediment sample (purified fraction). The abbreviations and nomenclature of maleimides is discussed in Section 3.1 and shown in Fig. A1.

Fig. 2. Two dimensional (2D) chromatograms obtained by two-dimensional gas chromatography (GC×GC) coupled to time-of-flight mass spectrometry (ToF-MS) for a) Si1 fraction and b) purified fraction of the McWhae Ridge MWR11 sample, and c) Si1 fraction and d) purified fraction of Lake Rotsee sample (CrO_3 oxidised extract) illustrating the extracted ion current of *m/z* 154, 168, 182, 196, 210, 224, and 238. e) Three dimensional (3D) chromatogram (surface plot) of maleimides as analysed by GC×GC-ToF-MS showing the extracted ion current of *m/z* 154, 168, 182, 210, 224, and 238 of the purified MWR11 sample. The relative amount of Me,Et maleimide in e) is underrepresented by exclusion of its characteristic fragment ion (*m/z* 196), due to its very high abundance. Names and abbreviations of illustrated maleimides are discussed in Section 3.1 and shown in Fig. A1.

Fig. 3. Schematic two dimensional (2D) chromatogram as analysed by two-dimensional gas chromatography (GC×GC) coupled to time-of-flight

mass spectrometry (ToF-MS) using the 1D and 2D retention times from Table 1 to illustrate retention times of all maleimides detected in this study without differences in their relative abundances. a) Scheme of complete 2D chromatogram. The peaks in the shaded area are magnified in b). Illustrated maleimides are shown in Fig. A1. b) Magnified 2D chromatogram illustrating maleimides in the *m/z* 210 (peaks A), 224 (peaks B), 238 (peaks C), 252 (peaks D) and 266 (peaks E). The corresponding maleimides are Me,*i*-Pr (C1), Et,Et (C2), Me,*n*-Pr (C3), H,*n*-Bu (C4; suggested structure), Et,*i*-Pr (B1; suggested structure), Et,*n*-Pr (B2; suggested structure), Me,*i*-Bu (B3), Me,*n*-Bu (B4), H,*n*-Pent (B5; suggested structure), Me,*i*-Pent(1-3) (C1, C3 and C4; suggested structures), Me,*neo*-Pent (C2), Me,*n*-Pent (C5), H,*n*-Hex (C6; suggested structure), peaks 1-5 of *m/z* 252 series (D1-D5), peaks 1-3 of *m/z* 266 series (E1-E3).

Fig. 4. Comparison of mass spectra of 2-methyl-3-ethyl-maleimide (Me,Et maleimide) analysed by a) gas chromatography – mass spectrometry (GC-MS) and b) two-dimensional gas chromatography coupled to time-of-flight mass spectrometry (GC×GC-ToF-MS). Also mass spectra of 2-methyl-3-*iso*-butyl-maleimide (Me,*i*-Bu maleimide) obtained by c) GC-MS and d) GC×GC-ToF-MS are illustrated. The mass spectra of all maleimides obtained with both instruments are shown in Figs. S1 and S2.

Fig. 5. Correlation between maleimide concentrations analysed by gas chromatography – mass spectrometry (GC-MS) and two-dimensional gas chromatography coupled to time-of-flight mass spectrometry (GC×GC-ToF-MS) using a) total ion current (TIC), b) *m/z* 75 or c) characteristic base peaks for quantification in the purified fraction of the MWR11 (McWhae Ridge) sample, d) using base peaks in the MWR13A sample and e) Lake Rotsee sample. Correlations of maleimides in the MWR11 and 13A samples f) including or g) excluding the concentrations of 2-methyl-3-ethyl-maleimide (Me,Et maleimide) using base peaks. Comparison of maleimide concentrations in the Si1 and purified fractions obtained by GC×GC-ToF-MS analysis using characteristic base peaks in h) MWR11 and i) MWR13A samples. The regression functions and correlation coefficient (R^2) values are also shown. The *m/z* of the characteristic base peaks used for quantification of the respective maleimides are listed in Section 2.3 and Table 1.

Fig. 6. Two dimensional (2D) chromatograms obtained by two-dimensional gas chromatography coupled to time-of-flight mass spectrometry (GC×GC-ToF-MS) analysis of the purified fraction of the MWR11 sample resolving coelution of maleimides with unknown compounds using the intensity of a) *m/z* 75 fragment and b) base peak fragment for H,H (*m/z* 154), Me,H (*m/z* 168), Me,*n*-Bu (*m/z* 224) and Me,*n*-Pent (*m/z* 238) maleimides for quantification.

Appendix

Fig. A1. Structures of maleimides detected in this study. Maleimides were named and abbreviated (details in Section 3.1) according to the nomenclature in [19,29]. The compounds indicated with a star (*) correspond to preliminarily assigned structures.

Fig 1

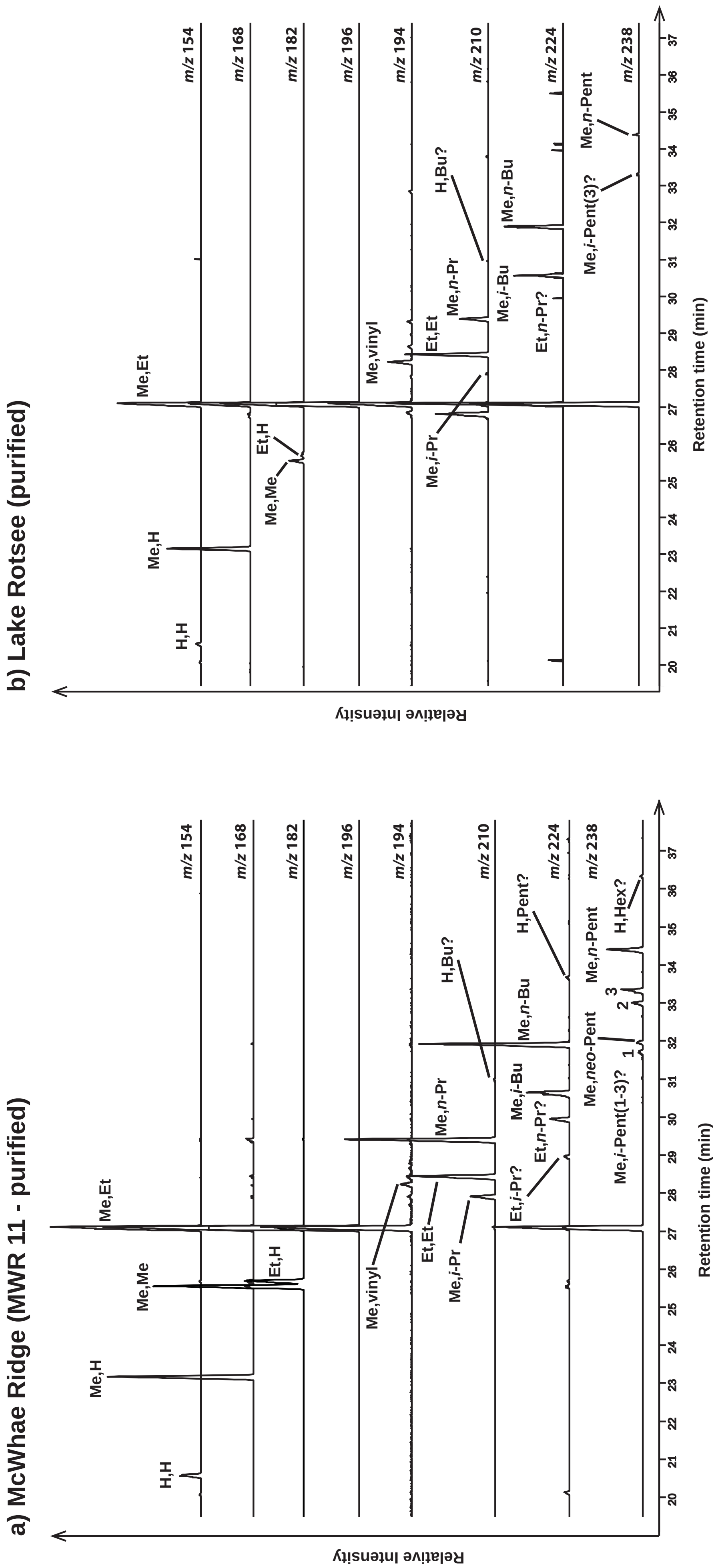

b) Lake Rotsee (purified)
a) McWhae Ridge (MWR 11 - purified)
Relative Intensity
Retention time (min)
20 21 22 23 24 25 26 27 28 29 30 31 32 33 34 35 36 37
m/z 154
m/z 168
m/z 182
m/z 196
m/z 194
m/z 210
m/z 224
m/z 238
H,H
Me,H
Me,Me
Et,H
Me,Et
Me,vinyl
Et,Et
Me,i-Pr
Me,n-Pr
H,Bu?
Me,i-Bu
Me,n-Bu
Et,n-Pr?
Et,i-Pr?
Me,i-Pent(3)?
Me,n-Pent
Me,i-Pent(1-3)?
Me,neo-Pent
H,Pent?
H,Hex?
1
2
3

Fig 2

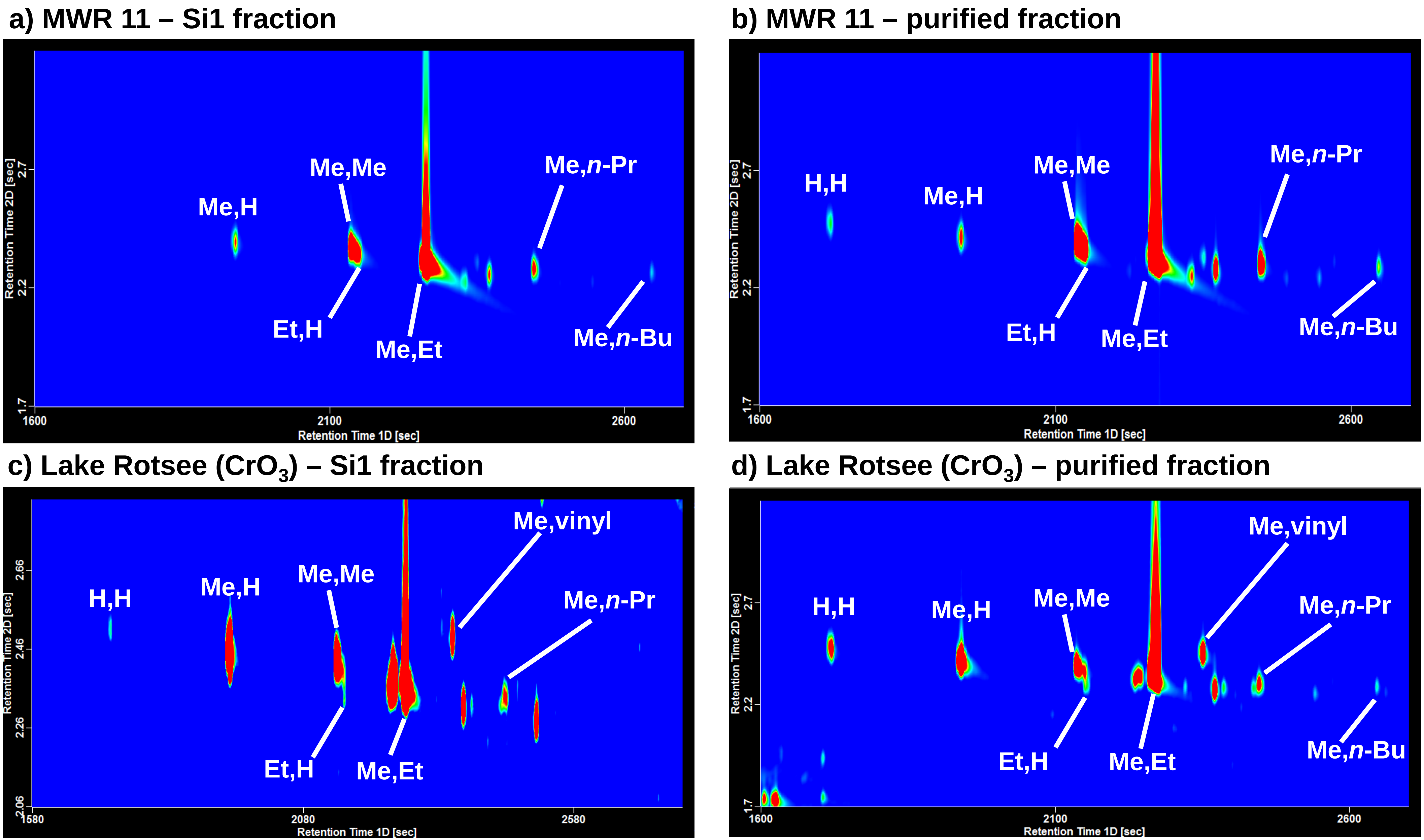

a) MWR 11 – Si1 fraction
Me,H
Me,Me
Et,H
Me,Et
Me,n-Pr
Me,n-Bu
Retention Time 2D [sec]
1.7
2.2
2.7
1600
2100
2600
Retention Time 1D [sec]
b) MWR 11 – purified fraction
H,H
Me,H
Me,Me
Et,H
Me,Et
Me,n-Pr
Me,n-Bu
Retention Time 2D [sec]
1.7
2.2
2.7
1600
2100
2600
Retention Time 1D [sec]
c) Lake Rotsee (CrO_3) – Si1 fraction
H,H
Me,H
Me,Me
Et,H
Me,Et
Me,vinyl
Me,n-Pr
Retention Time 2D [sec]
2.06
2.26
2.46
2.66
1580
2080
2580
Retention Time 1D [sec]
d) Lake Rotsee (CrO_3) – purified fraction
H,H
Me,H
Me,Me
Et,H
Me,Et
Me,vinyl
Me,n-Pr
Me,n-Bu
Retention Time 2D [sec]
1.7
2.2
2.7
1600
2100
2600
Retention Time 1D [sec]

Fig 2(e)

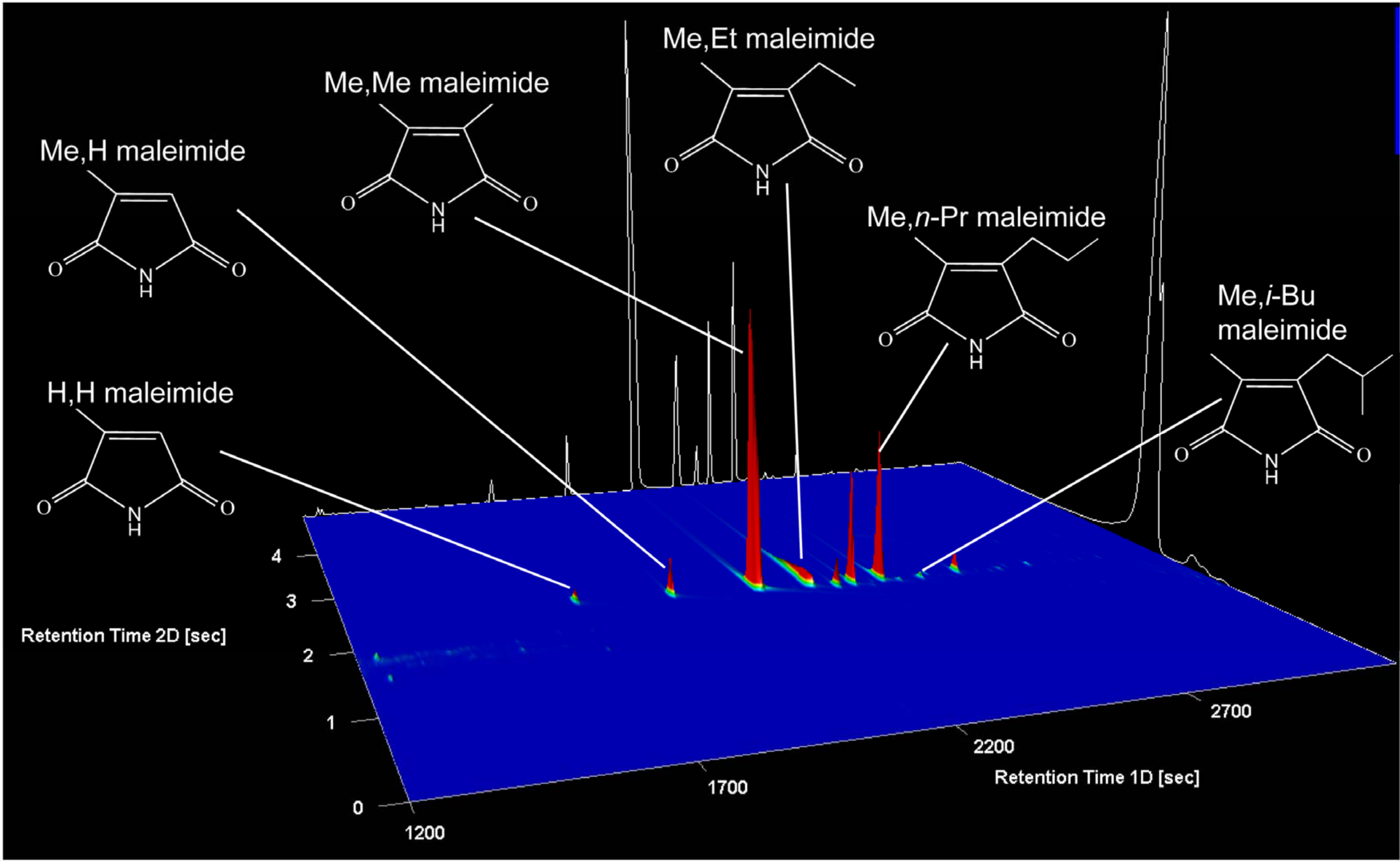
Me,Et maleimide
Me,Me maleimide
Me,H maleimide
Me,n-Pr maleimide
Me,i-Bu maleimide
H,H maleimide
Retention Time 2D [sec]
4
3
2
1
0
1200
1700
2200
2700
Retention Time 1D [sec]

FIG 3 (a)

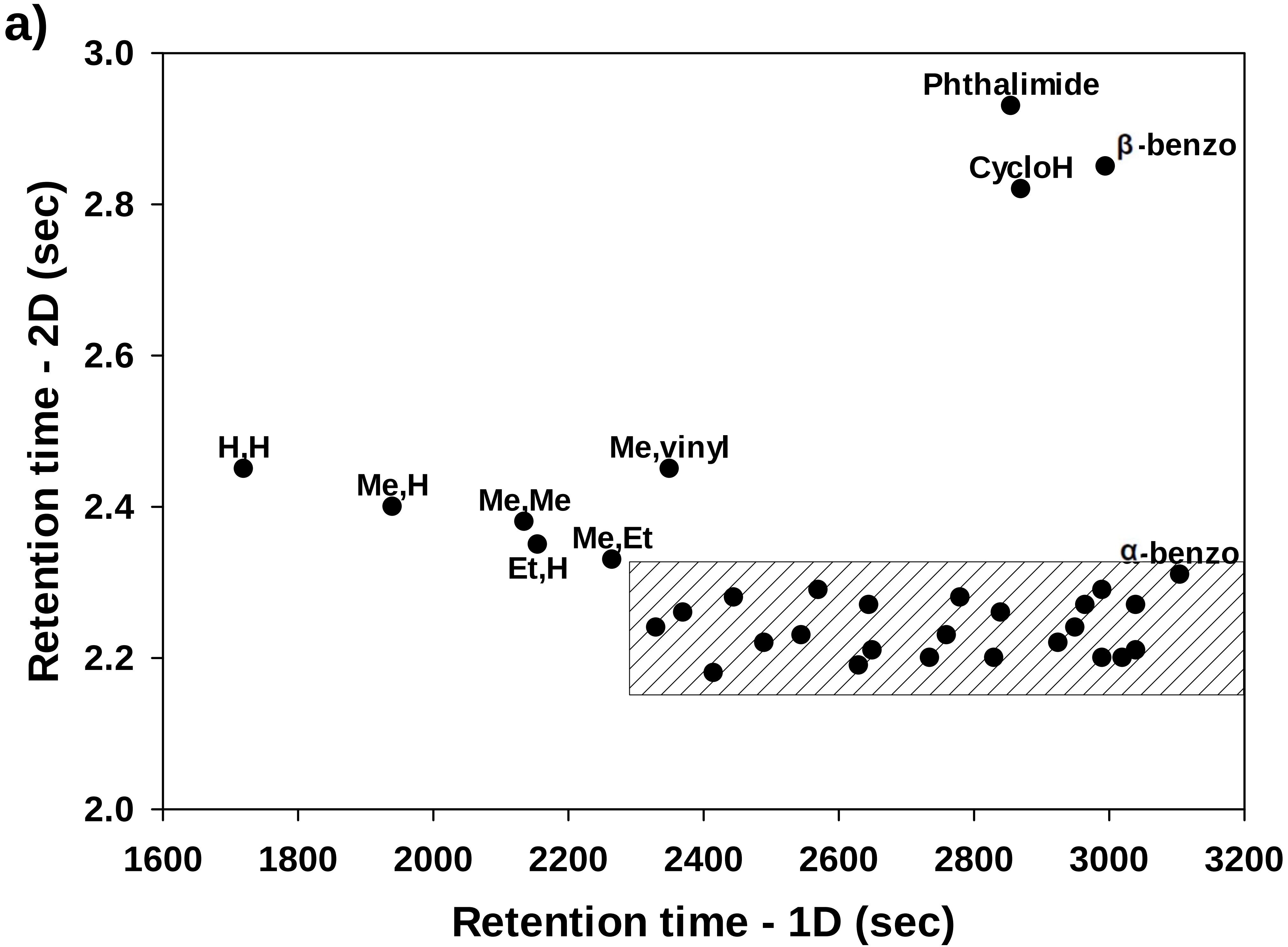

a)
Phthalimide
β-benzo
CycloH
H,H
Me,vinyl
Me,H
Me,Me
Me,Et
Et,H
α-benzo
3.0
2.8
2.6
2.4
2.2
2.0
1600
1800
2000
2200
2400
2600
2800
3000
3200
Retention time - 2D (sec)
Retention time - 1D (sec)

fig 3(b)

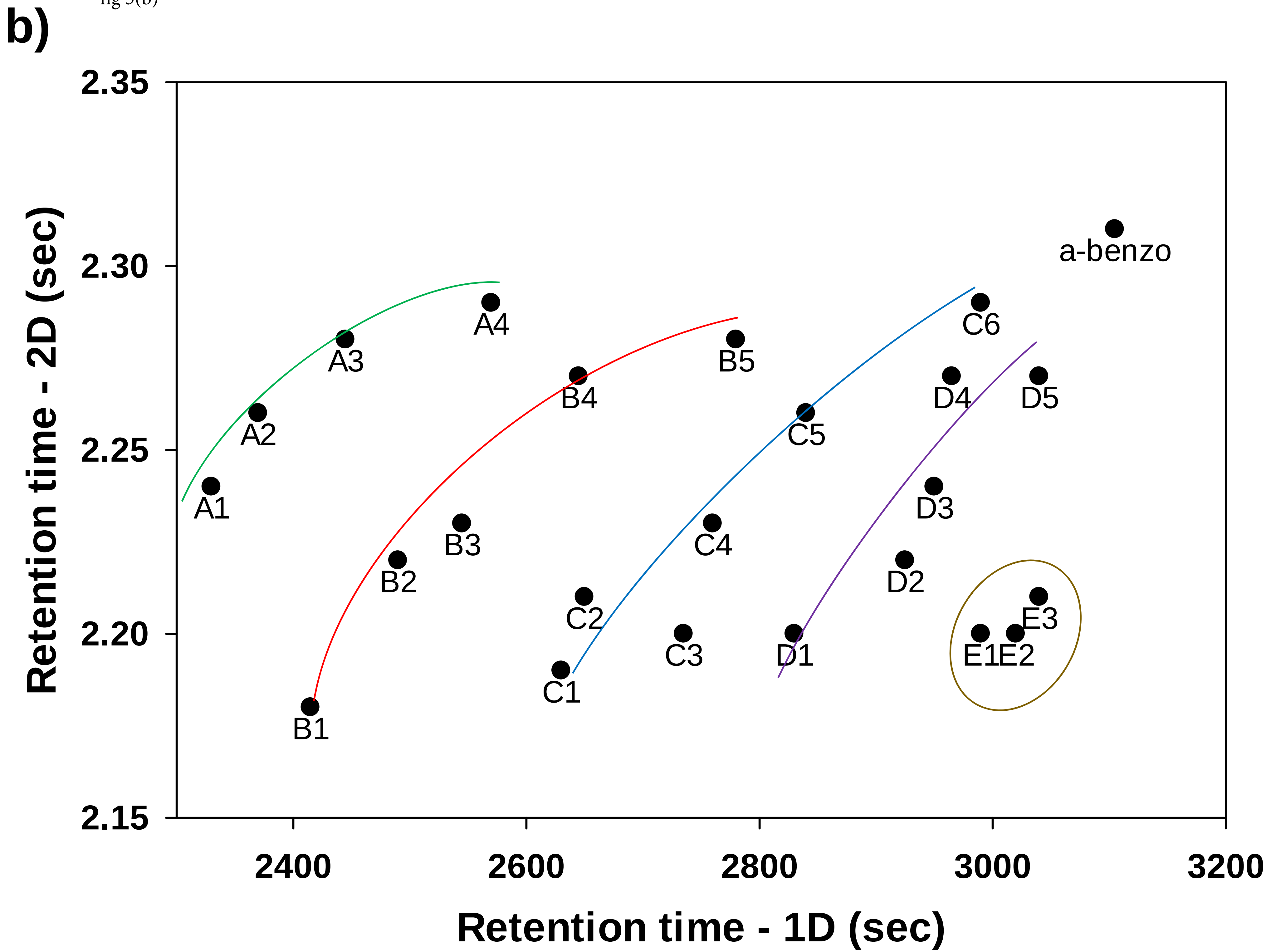
b)
Retention time - 2D (sec)
2.35
2.30
2.25
2.20
2.15
Retention time - 1D (sec)
2400
2600
2800
3000
3200
A1
A2
A3
A4
B1
B2
B3
B4
B5
C1
C2
C3
C4
C5
C6
D1
D2
D3
D4
D5
E1
E2
E3
a-benzo

fig 4

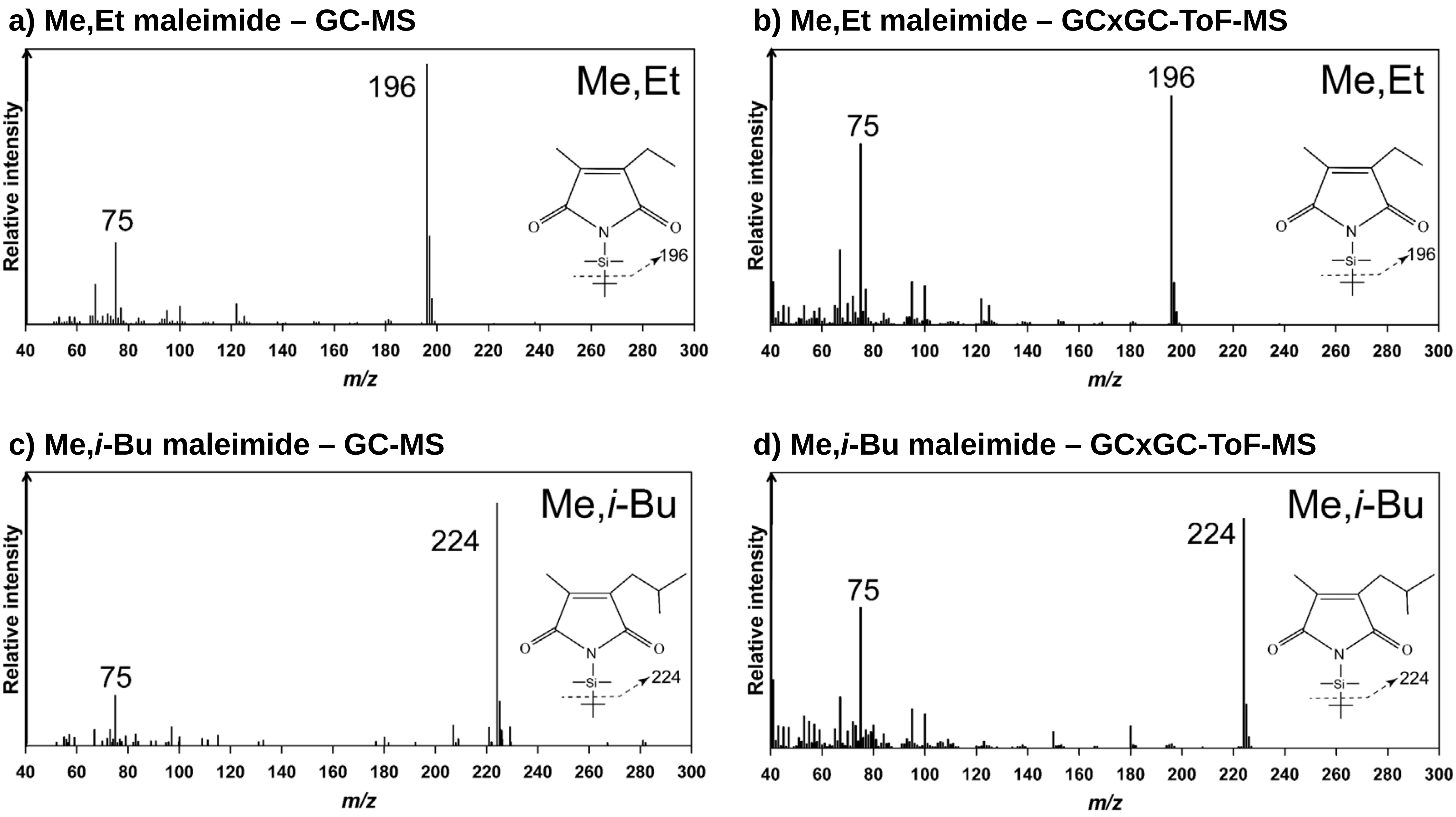
a) Me,Et maleimide – GC-MS
Me,Et
196
75
Relative intensity
m/z
b) Me,Et maleimide – GCxGC-ToF-MS
Me,Et
196
75
Relative intensity
m/z
c) Me,i-Bu maleimide – GC-MS
Me,i-Bu
224
75
Relative intensity
m/z
d) Me,i-Bu maleimide – GCxGC-ToF-MS
Me,i-Bu
224
75
Relative intensity
m/z

fig 5

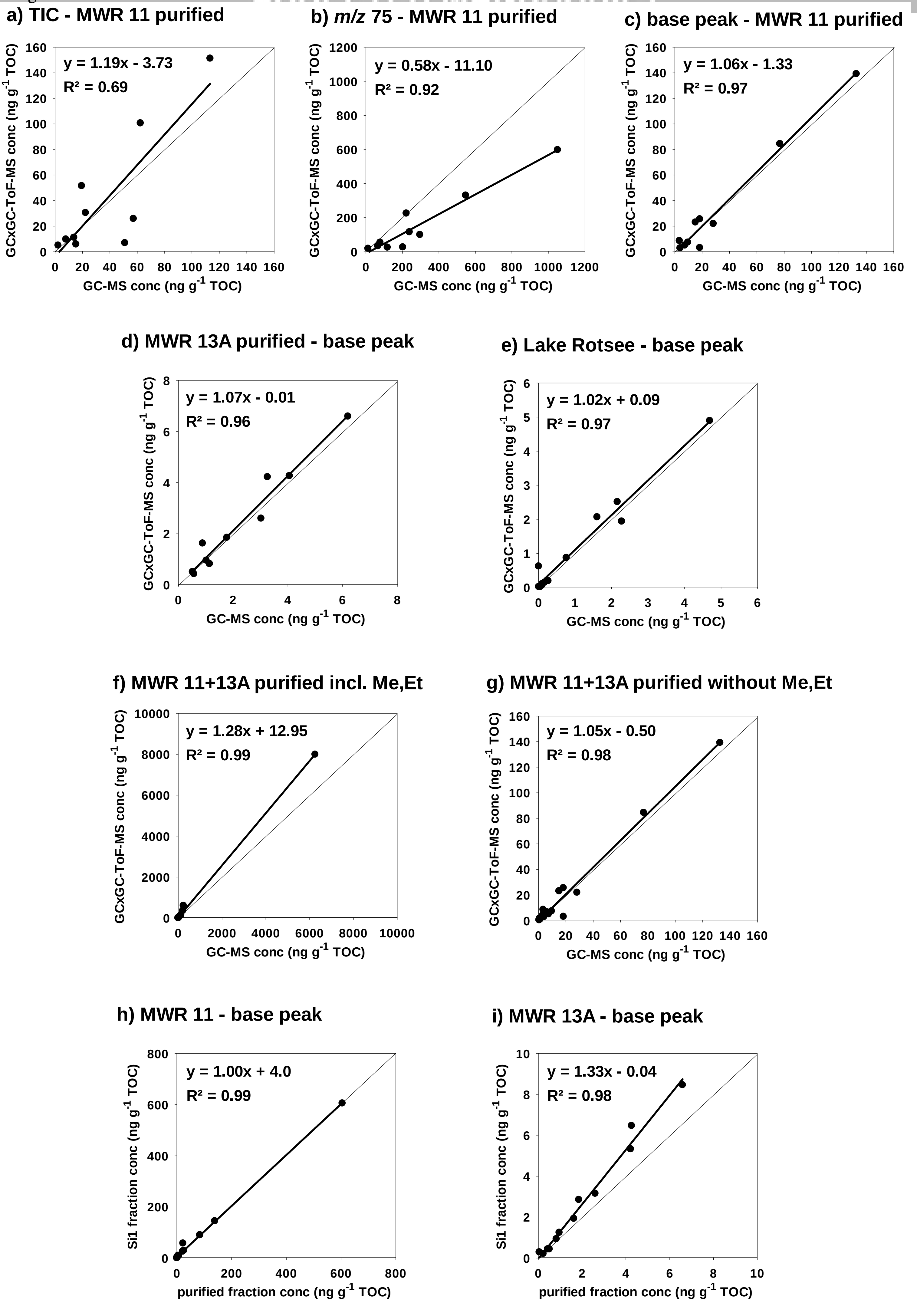

a) TIC - MWR 11 purified
y = 1.19x - 3.73
R² = 0.69
GCxGC-ToF-MS conc (ng g-1 TOC)
GC-MS conc (ng g-1 TOC)
b) m/z 75 - MWR 11 purified
y = 0.58x - 11.10
R² = 0.92
GCxGC-ToF-MS conc (ng g-1 TOC)
GC-MS conc (ng g-1 TOC)
c) base peak - MWR 11 purified
y = 1.06x - 1.33
R² = 0.97
GCxGC-ToF-MS conc (ng g-1 TOC)
GC-MS conc (ng g-1 TOC)
d) MWR 13A purified - base peak
y = 1.07x - 0.01
R² = 0.96
GCxGC-ToF-MS conc (ng g-1 TOC)
GC-MS conc (ng g-1 TOC)
e) Lake Rotsee - base peak
y = 1.02x + 0.09
R² = 0.97
GCxGC-ToF-MS conc (ng g-1 TOC)
GC-MS conc (ng g-1 TOC)
f) MWR 11+13A purified incl. Me,Et
y = 1.28x + 12.95
R² = 0.99
GCxGC-ToF-MS conc (ng g-1 TOC)
GC-MS conc (ng g-1 TOC)
g) MWR 11+13A purified without Me,Et
y = 1.05x - 0.50
R² = 0.98
GCxGC-ToF-MS conc (ng g-1 TOC)
GC-MS conc (ng g-1 TOC)
h) MWR 11 - base peak
y = 1.00x + 4.0
R² = 0.99
Si1 fraction conc (ng g-1 TOC)
purified fraction conc (ng g-1 TOC)
i) MWR 13A - base peak
y = 1.33x - 0.04
R² = 0.98
Si1 fraction conc (ng g-1 TOC)
purified fraction conc (ng g-1 TOC)

FIG 6

a)

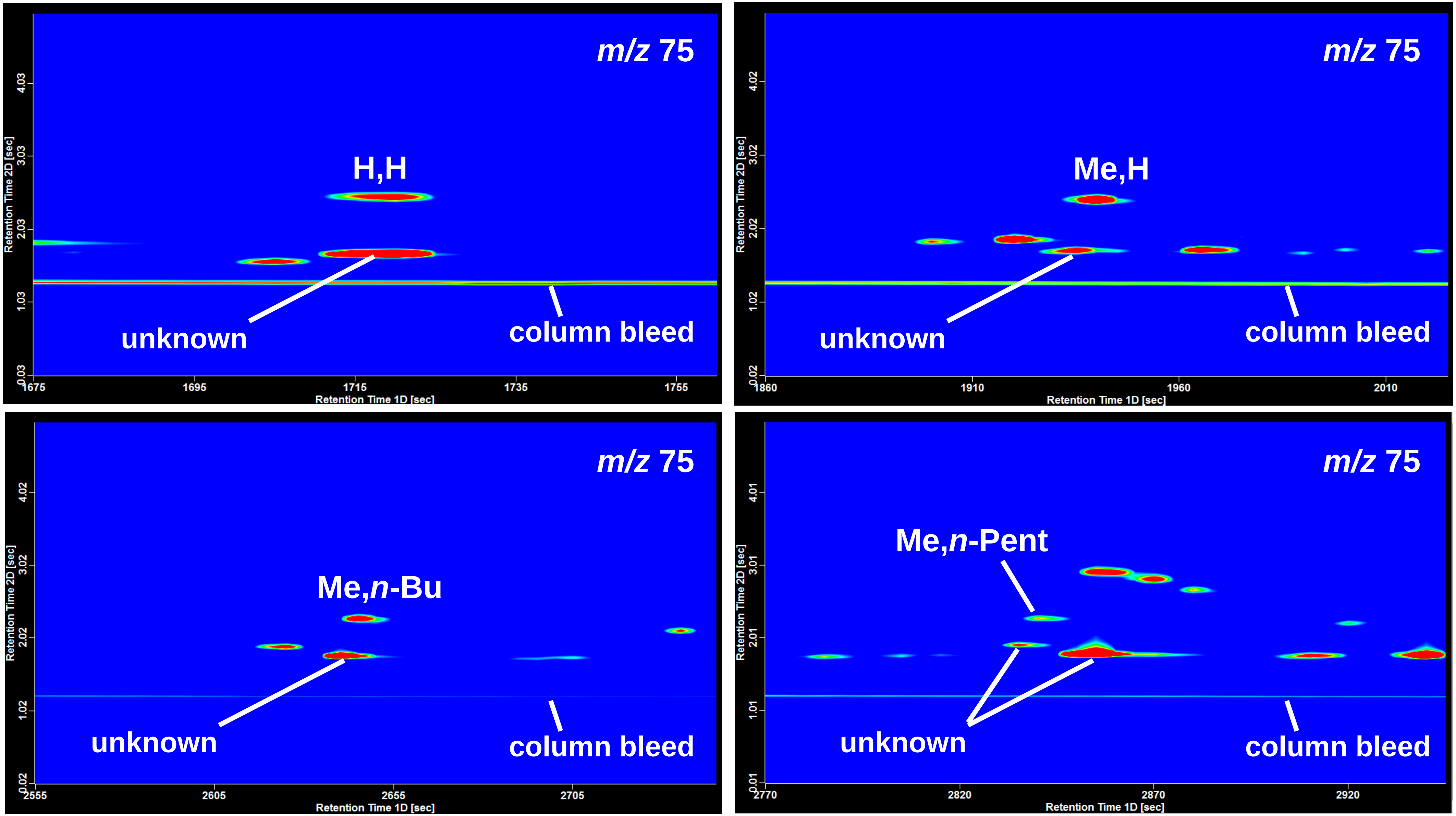
m/z 75
H,H
unknown
column bleed
Retention Time 2D [sec]
Retention Time 1D [sec]
m/z 75
Me,H
unknown
column bleed
m/z 75
Me,n-Bu
unknown
column bleed
m/z 75
Me,n-Pent
unknown
column bleed

b)

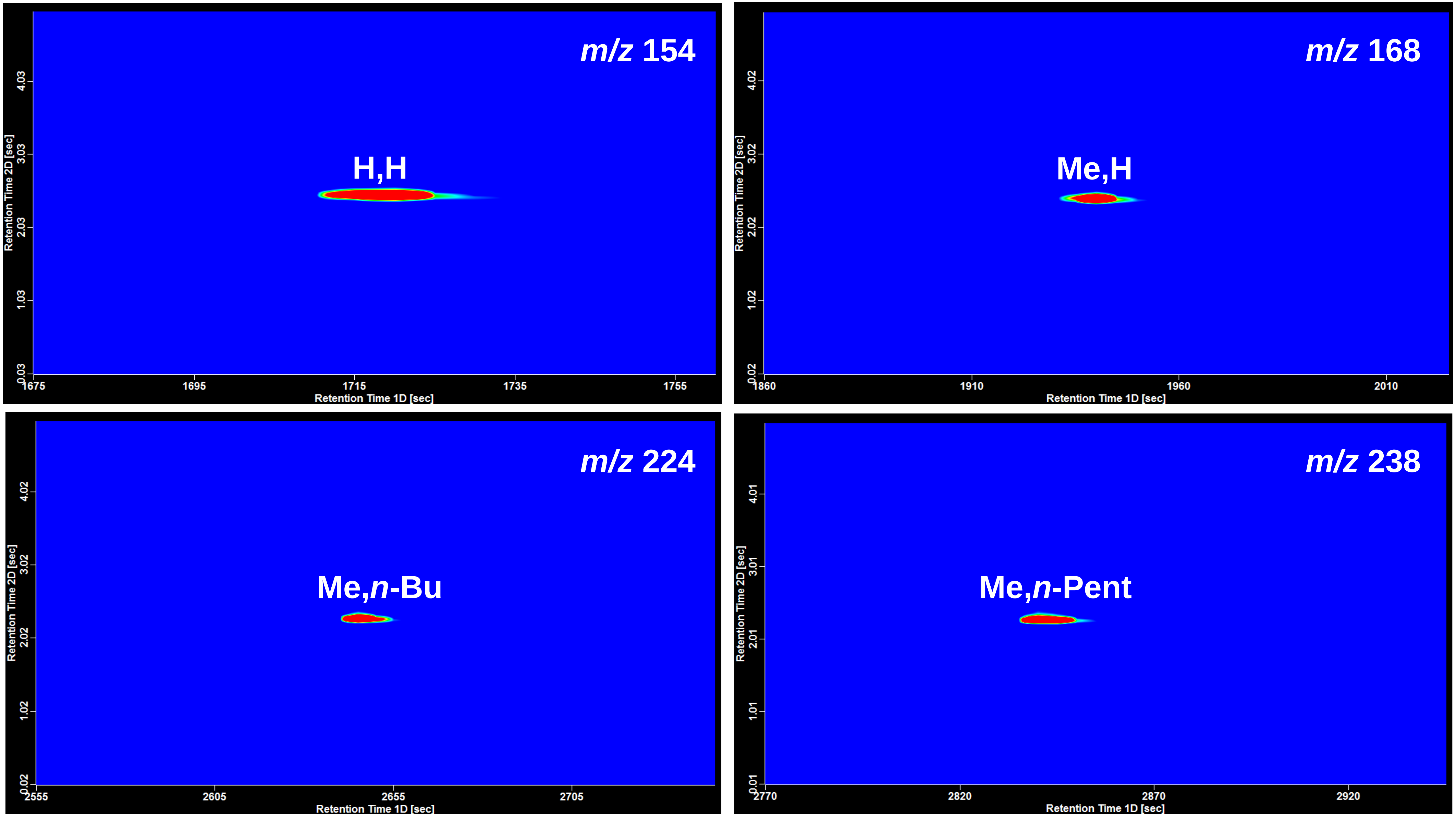

m/z 154
H,H
Retention Time 2D [sec]
Retention Time 1D [sec]
m/z 168
Me,H
m/z 224
Me,n-Bu
m/z 238
Me,n-Pent

Fig appendix 1